The Canadian Mineralogist
Vol. 33, pp. 1189-1204 (1995)

ENTROPY-DRIVEN DISORDER IN END-MEMBER AMPHIBOLES

FRANK C. HAWTHORNE

Department of Geological Sciences, University of Manitoba, Winnipeg, Manitoba R3T 2N2

ABSTRACT

The synthesis and characterization of end-member monoclinic amphiboles are reviewed, with a focus on chemical composition and order–disorder of cations over nonequivalent sites in the amphibole structure. Synthetic end-member amphiboles that have been characterized by physical or chemical methods in addition to optical examination and powder X-ray diffraction are tremolite, fluor-tremolite, actinolite, pargasite, fluor-pargasite, M^{3+}-substituted pargasite and fluor-pargasite (M^{3+} = Al, Cr^{3+}, Ga, Sc), ferro-pargasite, magnesio-hastingsite, hastingsite, richterite, potassium-richterite and ferro-richterite. In none of these cases was an ordered end-member amphibole of ideal composition synthesized; the amphiboles are either off-composition, or show unusual cation disorder, or both. Where analogous natural compositions occur, they seem to show similar features. These unusual schemes of order or unusual compositions are not present (or as prevalent) in synthetic and natural amphiboles of intermediate composition. Such intermediate compositions are also characterized by Mg–Fe^{2+} and Al–Fe^{3+} order–disorder relations that provide a significant contribution of configurational entropy to the energetics of the structure, a contribution that is absent from an ordered end-member amphibole of ideal composition. I propose that end-member or close-to-end-member amphiboles commonly show *entropy-driven disorder* that is required for their occurrence as stable structures. This disorder may occur as unusual site-populations, as small deviations from ideal end-member composition, or possibly as stacking disorder.

Keywords: amphibole, synthesis, order–disorder relation, entropy.

SOMMAIRE

La synthèse et la caractérisation des pôles des amphiboles monocliniques sont passées en revue, avec une attention particulière à la composition chimique et aux relations ordre–désordre des cations sur les sites non équivalents de la structure. Les pôles suivants des amphiboles synthétiques ont été décrits par leurs attributs physiques et chimiques, ainsi que par un examen de leurs propriétés optiques et par leur spectre de diffraction X (méthode des poudres): trémolite, fluor-trémolite, actinolite, pargasite, fluor-pargasite, pargasite et fluor-pargasite contenant des cations M^{3+} (M^{3+}: Al, Cr^{3+}, Ga, Sc), ferro-pargasite, magnésio-hastingsite, hastingsite, richterite, potassium-richterite et ferro-richterite. Dans aucun de ces cas est-il possible de synthétiser une amphibole ordonnée de composition idéale; les amphiboles résultantes ont soit une composition décalée de la composition idéale, soit un degré d'ordre inusité, ou les deux à la fois. Dans les cas où on trouve dans la nature des compositions analogues, elles semblent montrer des caractéristiques semblables. Ces schémas de mise en ordre ou de composition inusitées ne sont pas présents ou, du moins, aussi répandus dans les amphiboles synthétiques et naturelles de composition intermédiaire. De telles compositions intermédiaires ont aussi des schémas de mise en ordre Mg–Fe^{2+} et Al–Fe^{3+} qui contribuent de façon importante par l'entropie configurationnelle, à l'énergie de la structure, contribution qui est nulle dans le cas des amphiboles ordonnées dont la composition est celle d'un pôle. A mon avis, il est courant que les amphiboles proches de la composition d'un pôle montrent un désordre causé par l'entropie, nécessaire pour en stabiliser la structure. Ce désordre pourrait se manifester par une répartition inusitée des cations sur les sites, une légère déviation de la composition idéale, ou peut-être un désordre d'empilement.

(Traduit par la Rédaction)

Mots-clés: amphibole, synthèse, relation ordre–désordre, entropie.

INTRODUCTION

Systematic work on amphibole synthesis began in the late 1950s (Boyd 1959), and fairly extensive work throughout the following decade initially seemed to be quite successful. Amphiboles were synthesized, and their fields of stability were examined as a function of T (temperature), P (Pressure) and $f(O_2)$ (oxygen fugacity) (Ernst 1968). The run products of such studies were usually examined only by optical microscopy and powder X-ray diffraction; amphiboles were assumed to be of nominal composition, and additional phases were ignored or considered metastable. These statements are *not* meant to be pejorative; without this pioneering work, subsequent studies would not have been possible. However, examination of products of amphibole synthesis in the 1970s and 1980s showed the resultant amphibole to differ in subtle ways from what was expected to grow. As the sophistication of the available methods of characterization increased (Hawthorne 1983), further work over the last ten years has confirmed the fact that it is very difficult to synthesize the amphibole one expects from a specific starting composition. Here, I critically review available information on the synthesis and characterization of nominally end-member amphibole compositions, and compare these findings with analogous information on natural amphiboles. In some cases, recent work on natural amphiboles has shown that previous expectations concerning the patterns of order in end-member amphiboles were wrong, and that synthetic amphiboles *are* similar to their natural analogues. Recent comprehensive studies of amphibole synthesis are reported by Graham *et al.* (1989) and Raudsepp *et al.* (1991). The departure of synthetic end-member amphiboles from their ideal composition and state of order has been previously emphasized by Hawthorne (1983) and Graham *et al.* (1989), who suggested additional methods of run-product characterization. Here, I examine some of the relevant information and suggest an explanation for the departure of synthetic end-member amphiboles from their ideal composition and state of order.

CALCIC AMPHIBOLES

Tremolite

Tremolite has been synthesized by numerous authors (Boyd 1959, Troll & Gilbert 1972, Wones & Dodge 1977, Oba 1980, Skippen & McKinstry 1985, Jenkins 1987, Cho & Ernst 1991, Pawley *et al.* 1993). However, as noted by Jenkins (1987), none of these studies has reported complete yields of tremolite; most quote yields of ~90 wt% tremolite and 10 wt% diopside, with or without quartz. Very careful work by Jenkins (1987) along the pseudobinary join $Mg_7Si_8O_{22}(OH)_2$–$Ca_2Mg_5Si_8O_{22}(OH)_2$ suggested the phase relations shown in Figure 1. Synthetic tremolite does not seem to be stable at its ideal composition, $Ca_2Mg_5Si_8O_{22}(OH)_2$, but contains a significant amount (5–10%) of $Mg_7Si_8O_{22}(OH)_2$ in solid solution. In terms of the amphibole structure, this indicates a significant amount of Mg at the *M*(4) site. Jenkins (1987) and Jenkins *et al.* (1991) also showed that hydrothermal treatment of natural tremolite can lead to its incongruent dissolution *via* the reactions

$$\text{tremolite} \rightleftharpoons \text{orthopyroxene} + \text{clinopyroxene} + SiO_2(aq) + H_2O \quad (1)$$

$$\text{tremolite} \rightleftharpoons \text{forsterite} + \text{clinopyroxene} + SiO_2(aq) + H_2O \quad (2)$$

that depend on the degree of silica undersaturation in the aqueous fluid. Reaction (1) occurs in mildy undersaturated fluids, and reaction (2) occurs in strongly undersaturated fluids. However, tremolite synthesis with quartz-excess compositions still gave tremolite compositions with significant Mg at the *M*(4) site.

Jenkins (1987) also examined the composition of natural amphiboles close to that of ideal end-member tremolite, and showed that *none* corresponds to ideal tremolite according to the criterion $Ca/\Sigma M = 0.40$. Natural compositions usually have $Ca/\Sigma M$ less than 0.40, which was taken as a measure of significant Mg (or Fe^{2+} or Mn^{2+}) at the *M*(4) site. In this regard, it should be emphasized that use of the quantity $Ca/\Sigma M$ as a measure of departure or adherence to the ideal end-member composition is not justified, as it ignores the fact that Ca may occur at the *A* site in both synthetic (Boschmann *et al.* 1994, Oberti *et al.* 1995b) and natural (Hawthorne *et al.* 1995) amphiboles. In addition, it does not recognize the presence of Na at the *A* site and Al at the *T* sites. Such compositional aspects of tremolite are better examined using the variables $^A(Na + K + Ca)$, $^B(Fe + Mn + Mg)$ and ^TAl (assuming that $^CMg = 5$ atoms per formula unit, *apfu*). Graham *et al.* (1989) contested the idea that nominal end-member tremolite compositions do not occur, and cited the tremolite compositions of Kiseleva & Ogorodova (1984) and Welch (1987) as proof.

Ahn *et al.* (1991) have shown that synthetic tremolite also has significant populations of chain-width defects, the density of defects decreasing with increasing temperature of synthesis. This may be a kinetic issue, as Ahn *et al.* (1991) suggested that triple-chain silicate is an important precursor phase to amphibole, but it is also possible that it is a form of local disorder that is more effective at lower temperatures and is replaced by increasing Ca–Mg disorder as temperature increases.

Fluor-tremolite

Synthesis of fluor-tremolite has been reported by Cameron & Gibbs (1973), Graham & Navrotsky (1986) and Raudsepp *et al.* (1991), with yields varying from 80 to >95%. Cameron & Gibbs (1973) refined the structure of fluor-tremolite assuming ideal site-populations; however, they did not examine the possibility of Mg-for-Ca substitution at *M*(4), as occurs for synthetic tremolite. Raudsepp *et al.* (1991) analyzed their synthetic fluor-tremolite with an electron microprobe. The chemical composition and resulting formula unit (Table 1) show significant Mg at the *M*(4) site and a Ca content less than the ideal value of 2.0 *apfu*; the analysis also shows minor Al_2O_3 contamination from grinding the starting materials in a corundum mortar. Nevertheless, the situation seems to be analogous with synthetic and natural tremolite: significant Mg at the *M*(4) site.

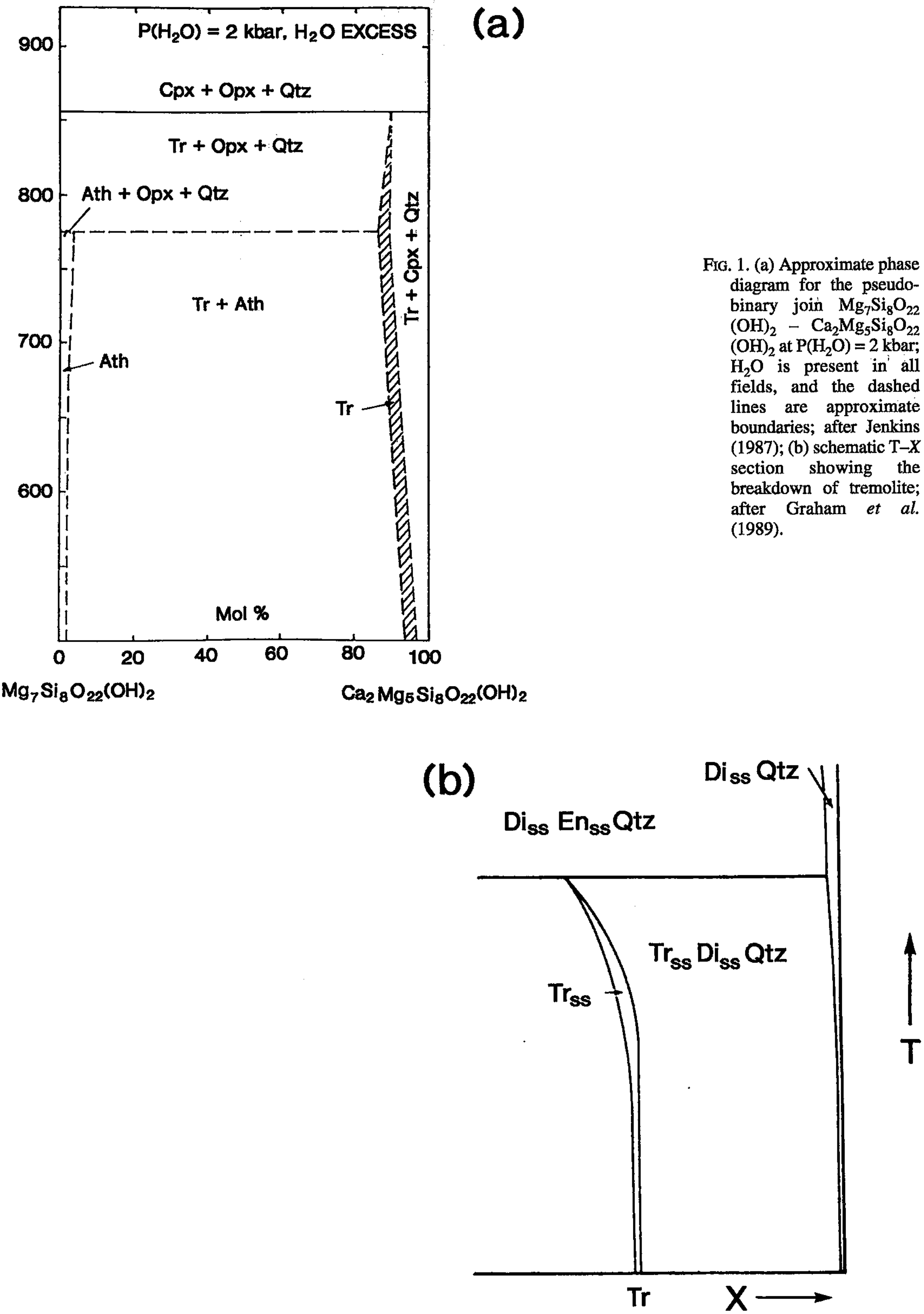

FIG. 1. (a) Approximate phase diagram for the pseudo-binary join $Mg_7Si_8O_{22}(OH)_2$ – $Ca_2Mg_5Si_8O_{22}(OH)_2$ at $P(H_2O) = 2$ kbar; H_2O is present in all fields, and the dashed lines are approximate boundaries; after Jenkins (1987); (b) schematic T–*X* section showing the breakdown of tremolite; after Graham *et al.* (1989).

TABLE 1. ELECTRON-MICROPROBE DETERMINATION OF THE COMPOSITION (wt%) AND *UNIT FORMULAE (APFU) OF SYNTHETIC AMPHIBOLES

	F-TREM	PARG	PARG	SC-PARG	F-PAR	SC-F-PAR	MG-HAS	SC-F-ECK	IN-F-ECK
SiO_2	58.06	42.48	43.18	44.79	41.39	41.57	41.8	58.53	54.60
Al_2O_3	0.67	18.12	18.19	13.96	17.67	12.20	12.1	0.26	0.24
Fe_2O_3	–	–	–	–	–	–	9.3	–	–
Sc_2O_3	–	–	–	3.39	–	7.35	–	8.34	–
In_2O_3	–	–	–	–	–	–	–	–	16.39
MgO	25.76	19.00	19.26	19.76	20.30	19.42	19.1	19.18	18.06
CaO	12.46	13.56	13.15	12.83	14.09	12.50	13.2	–	–
Na_2O	–	3.50	3.91	3.85	2.93	3.72	3.5	10.98	10.19
F	4.26	–	–	–	4.64	4.85	–	4.46	4.05
	101.21	96.66	97.69	98.58	100.92	101.61	99.0	101.75	103.52
O=F	1.79	–	–	–	1.91	2.04	–	1.88	1.71
	99.42	96.66	97.69	98.58	99.01	99.57	99.0	99.87	101.81
Si	7.93	5.99	6.02	6.22	5.86	5.94	5.95	8.04	8.02
Al	0.07	2.01	1.98	1.78	2.14	2.06	2.03	–	–
ΣT	8.00	8.00	8.00	8.00	8.00	8.00	7.98	8.04	8.02
Al	0.04	1.00	1.01	0.51	0.81	–	–	0.04	0.04
Fe^{3+}	–	–		–	–	–	1.00	–	–
Sc	–	–		0.41	–	0.92	–	1.00	–
In	–	–		–	–	–	–	–	1.04
Mg	4.96	3.99	3.99	4.08	4.19	4.08	4.05	3.93	3.92
ΣC	5.00	4.99	5.00	5.00	5.00	5.00	5.05	4.97	5.00
Mg	0.28	–	–	0.01	0.10	0.06	–	–	0.03
Ca	1.82	2.05	1.96	1.91	2.06	1.91	2.01	–	–
Na	–	–	0.04	0.08	–	0.03	–	2.00	1.97
ΣB	2.10	2.05	2.00	2.00	2.16	2.00	2.01	2.00	2.00
Na^A	–	0.96	1.02	0.96	0.80	1.00	0.97	0.92	0.93
Ref.	(1)	(1)	(2)	(1)	(1)	(1)	(3)	(1)	(1)

References: (1): Raudsepp *et al.* (1991); (2): Welch *et al.* (1994); (3) Semet (1973).
* calculated on the basis of 23 Ox pfu

Actinolite

Actinolite was synthesized by Ernst (1966), who also examined its stability relations. In no case was a complete yield of amphibole produced; one or more of the phases quartz, fayalite, hedenbergite and magnetite were always present in the run products. Ernst (1966) noted that the optical properties and cell dimensions were constant and did not depend on the percentage of amphibole present in the run product, and concluded that the amphibole synthesized does not show any solid solution with grunerite, $Fe_7Si_8O_{22}(OH)_2$.

Burns & Greaves (1971) recorded the Mössbauer spectrum of actinolite synthesized by Ernst (1966). In ideal ordered end-member actinolite, $Ca_2Fe^{2+}_5Si_8O_{22}(OH)_2$, the Mössbauer spectrum should consist of three quadrupole-split Fe^{2+} doublets with area ratios of 2:2:1, corresponding to Fe^{2+} at the *M*(1), *M*(2) and *M*(3) sites, respectively. Inspection of the Mössbauer spectrum of synthetic actinolite (Fig. 2) shows that this is not the case. The spectrum was fitted to three quadrupole-split doublets, the Mössbauer parameters of which are characteristic of octahedrally coordinated Fe^{2+}. However, the area ratios are certainly not 2:2:1 (Fig. 2). This could be, in part, due to the occurrence of other Fe-bearing phases in the run product. However, Burns & Greaves (1971) suggested that the anomalous area ratios are due to the occurrence of Fe^{2+} replacing Ca at the *M*(4) site, and this is in accord with the occurrence of Mg at *M*(4) in synthetic tremolite (Jenkins 1987).

Synthetic pargasite

Pargasite, ideally $NaCa_2(Mg_4Al)(Si_6Al_2)O_{22}(OH)_2$, has been synthesized by Boyd (1959), Charles (1980), Raudsepp *et al.* (1987a) and Welch *et al.* (1994). In no case was there a complete yield of amphibole, although yields greater than 95% are common. Electron-microprobe analysis of synthetic pargasite (Raudsepp *et al.* 1991, Welch *et al.* 1994) gave a composition (Table 1) that is almost ideal. The slight excess of Ca (0.05 *apfu*) and deficiency of Na (0.04 *apfu*) may be just random error, as the infrared spectrum in the principal OH-stretching region shows no sign of an *A*-site-vacant O(3) configuration (*cf.* richterite and potassium-richterite). In ideally ordered end-member pargasite, the site occupancies should be *M*(1) = *M*(3) = Mg, *M*(2) = MgAl. The OH anion occupies the O(3) site, which is coordinated by the *M*(1) (×2) and *M*(3) sites; thus in

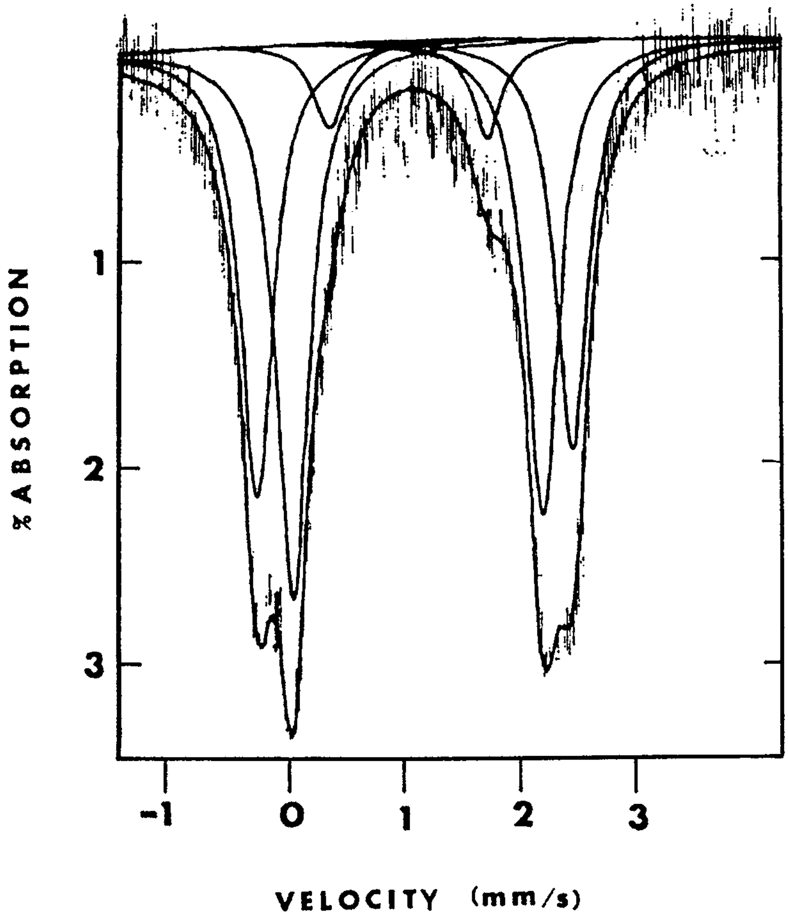

FIG. 2. The ^{57}Fe Mössbauer spectrum of synthetic ferro-actinolite; after Burns & Greaves (1971).

ideally ordered end-member pargasite, OH is coordinated by MgMgMg. This ordered arrangement should result in a single band in the principal OH-stretching region of the infrared spectrum. As is apparent in Figure 3a, this is not the case. The infrared spectrum of synthetic pargasite shows two bands of approximately equal intensity (given the uncertainty in defining the baseline of the spectrum); this indicates that Al occurs at one or both of the *M*(1) and *M*(3) sites. A similar result is obtained from the ^{1}H MAS NMR spectrum of pargasite (Welch *et al.* 1994). ^{27}Al MAS NMR and ^{27}Al–^{1}H CP MAS spectra (Fig. 3b) of pargasite (Welch *et al.* 1994) show two peaks due to $^{[6]}$Al, only one of which cross-polarizes. This indicates that some $^{[6]}$Al is adjacent to an OH group and some $^{[6]}$Al is not adjacent to an OH group; the former $^{[6]}$Al occupies one or both of the *M*(1) and *M*(3) sites, and the latter occupies the *M*(2) site. Thus the spectroscopic work on synthetic pargasite indicates that Al is disordered over at least two of the *M*(1), *M*(2) and *M*(3) sites.

Natural pargasite

Oberti *et al.* (1995a) refined the structure of 15 crystals of pargasite from the Finero mafic–ultramafic complex, Ivrea–Verbano Formation, Italy. The amphiboles have fairly low Fe contents ($2.9 < \text{FeO} < 8.4$ wt%) and hence approach end-member pargasite composition more closely than do most natural amphiboles. These amphiboles have octahedrally coordinated Al at the *M*(2) and *M*(3) sites, but not at the *M*(1) site. Furthermore, the amount of Al at *M*(3) increases with decreasing Fe content of the amphibole, and extrapolation to zero Fe-content suggests complete Al disorder over *M*(2) and *M*(3), as occurs for Sc in synthetic Sc-pargasite (Raudsepp *et al.* 1987a).

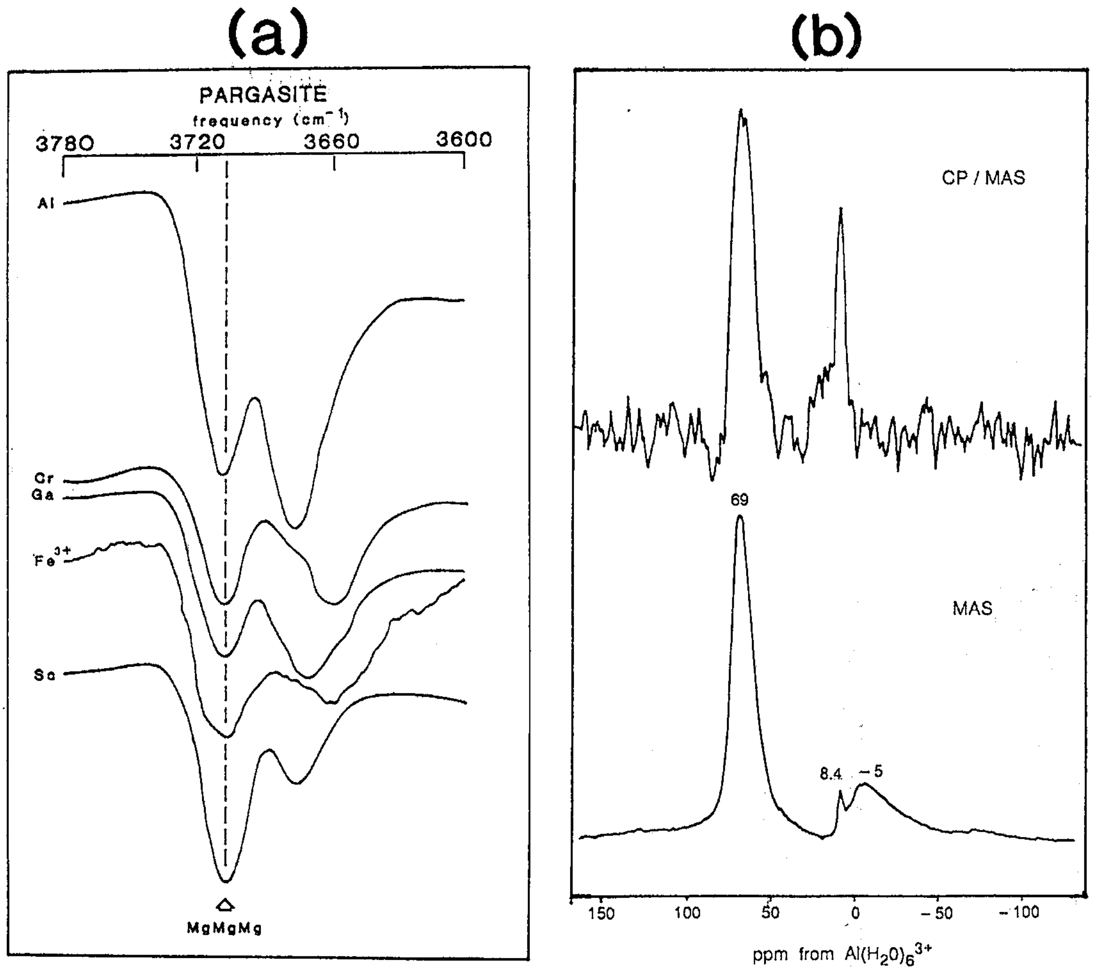

FIG. 3. (a) Infrared spectra in the principal OH-stretching region for synthetic amphiboles of the form $NaCa_2(Mg_4M^{3+})(Si_6Al_2)O_{22}(OH)_2$, where M^{3+} is indicated on the left of the spectra; spectra from Semet (1973) and Raudsepp *et al.* (1987a); (b) ^{27}Al MAS NMR spectra of synthetic pargasite; the upper spectrum is the ^{27}Al–^{1}H CP MAS spectrum. The intense peak at 69 ppm is due to $^{[4]}$Al, and the other peaks are due to $^{[6]}$Al. After Welch *et al.* (1994).

Synthetic M^{3+}-substituted pargasite

Raudsepp *et al.* (1987a) synthesized a series of pargasite compositions $NaCa_2(Mg_4M^{3+})(Si_6Al_2)O_{22}(OH)_2$, with M^{3+} representing Al, Cr^{3+}, Ga or Sc. The infrared spectra of these amphiboles (Fig. 3a) all show more than one band, indicative of trivalent cations at one or both of the *M*(1) and *M*(3) sites. Rietveld refinement of Sc-pargasite shows the *M*(1) site to be completely occupied by Mg, with Sc completely disordered over the *M*(2) and *M*(3) sites (the total Sc-content is also less than the ideal value of 1 *apfu*, Table 1). This pattern of ordering is the same as that observed in natural Fe-poor pargasite (Oberti *et al.* 1995a).

Fluor-pargasite and M^{3+}-substituted fluor-pargasite

Fluor-pargasite was synthesized by Westrich & Navrotsky (1981) and Raudsepp *et al.* (1987a, 1991). Yields are higher than for the hydroxyl analogue, but the results of electron-microprobe analysis (Table 1) show significant departures from ideal end-member stoichiometry. For the M^{3+}-substituted fluor-pargasite, the compositions of fluor-pargasite and scandium-fluor-pargasite are much closer to those of the ideal

TABLE 2. SITE OCCUPANCIES IN SELECTED SYNTHETIC AMPHIBOLES*

Scandium-pargasite				
M(1)	Mg	1.04(2)	Sc	−0.04(2)
M(2)	Mg	0.79(2)	Sc	0.21(2)
M(3)	Mg	0.79(3)	Sc	0.21(3)
Scandium-fluor-pargasite				
M(1)	Mg	0.92(1)	Sc	0.09(1)
M(2)	Mg	0.60(1)	Sc	0.40(1)
M(3)	Mg	1.00(2)	Sc	0.00(2)
Scandium-fluor-eckermannite				
M(1)	Mg	0.97(1)	Sc	0.03(1)
M(2)	Mg	0.57(1)	Sc	0.43(1)
M(3)	Mg	1.06(1)	Sc	−0.06(1)
Indium-fluor-eckermannite				
M(1)	Mg	1.00(1)	In	0.00(1)
M(2)	Mg	0.52(1)	In	0.48(1)
M(3)	Mg	1.00(1)	In	0.00(1)

* from Raudsepp *et al.* (1987a,b)

end-members (Table 1), and Rietveld refinement (Table 2) shows the trivalent cation to be almost completely ordered at the *M*(2) site (*i.e.*, not coordinated by F). Nevertheless, although the F end-members are more ordered than their OH analogues, they do depart significantly from ideal end-member composition.

Ferro-pargasite

Ferro-pargasite has been synthesized by Gilbert (1966) and Charles (1980); in no case did yields approach 100% amphibole, and Charles reported a few % to about 30% by volume of pyroxene and plagioclase in run products along the pargasite – ferro-pargasite join. Gilbert (1966) recorded a regular decrease in cell volume with increase in oxygen fugacity of synthesis, from 928.5 Å^3 on the IW buffer to 925.4 Å^3 on the Ni–NiO buffer, and ascribed this to an increase in the amount of Fe^{3+} with increasing oxygen fugacity of synthesis. On the other hand, Charles (1980) reported no difference between the cell volumes of ferro-pargasite synthesized on the QFM and CCH_4 buffers, so the situation here with regard to possible variation in Fe^{3+} content is not clear. There is no information on any order–disorder effects, but certainly the low yields do suggest deviation from ideal composition.

Magnesio-hastingsite

The synthesis and characterization of magnesio-hastingsite, ideally $NaCa_2(Mg_4Fe^{3+})(Si_6Al_2)O_{22}(OH)_2$, were reported by Semet (1973). Amphibole yields varied between 90 and 100%, and repeated grinding and recrystallization led to yields containing "virtually only one amphibole" (Semet 1973). Cell dimensions and indices of refraction decrease with increasing oxygen fugacity of synthesis, indicating that the amphibole is generally not "on composition", despite the near-100% yields of amphibole. Mössbauer spectra were recorded for magnesio-hastingsite synthesized on all buffers; Fe^{2+} was present at all conditions except for those compositions equilibrated at the cuprite–tenorite buffer (Fig. 4a). Thus all amphiboles synthesized are off-composition, with the possible exception of that synthesized at the highest oxygen fugacity, which has a chemical composition (Table 1) virtually identical to ideal end-member magnesio-hastingsite. The infrared spectrum of this specific end-member magnesio-hastingsite (Fig. 3) shows significant occupancy of the *M*(1) + *M*(3) sites by Fe^{3+}. Hence, although magnesio-hastingsite synthesized on the cuprite–tenorite buffer has ideal end-member composition, it has partial Fe^{3+} disorder over the *M*(1), *M*(2) and *M*(3) sites, and does not correspond to the ideal ordered end-member.

Hastingsite

Hastingsite was synthesized by Thomas (1982a). In no case did 100% yield of amphibole occur, and accompanying phases included hedenbergite, fayalite, nepheline, magnetite and plagioclase. Thomas (1982a) reported that the cell dimensions decrease slightly with increasing oxygen fugacity of synthesis, and suggested that this denotes increasing Fe^{3+} content (and therefore varying composition) with increasing oxygen fugacity of synthesis. Thomas (1982b) reported a detailed Mössbauer study of synthetic hastingsite. Ideally ordered end-member hastingsite should have the following site occupancies: *M*(1) = *M*(3) = Fe^{2+}, *M*(2) = Fe^{2+}Fe^{3+}; hence the corresponding Mössbauer spectrum should have three quadrupole-split Fe^{2+} doublets and one quadrupole-split Fe^{3+} doublet with area ratios 2:1:1:1, respectively. The spectrum of hastingsite synthesized on the wüstite–magnetite buffer is shown in Figure 5. Four-doublet fits (Fig. 5) gave area ratios inconsistent with the expected area-ratios. Three-doublet fits (not shown) gave slightly more consistent results, if one assumes that the *M*(1) and *M*(3) doublets overlap *and* that all Fe^{3+} is ordered at *M*(2); however, Thomas (1982b) did not consider this assignment as conclusive. An infrared study of these hastingsite samples would have proved interesting. The Fe^{3+}/Fe^{2+} derived from the fitting process should be reasonably independent of the model used for fitting of the Fe^{2+} doublets. The Fe^{3+} area ratio is 0.20 for end-

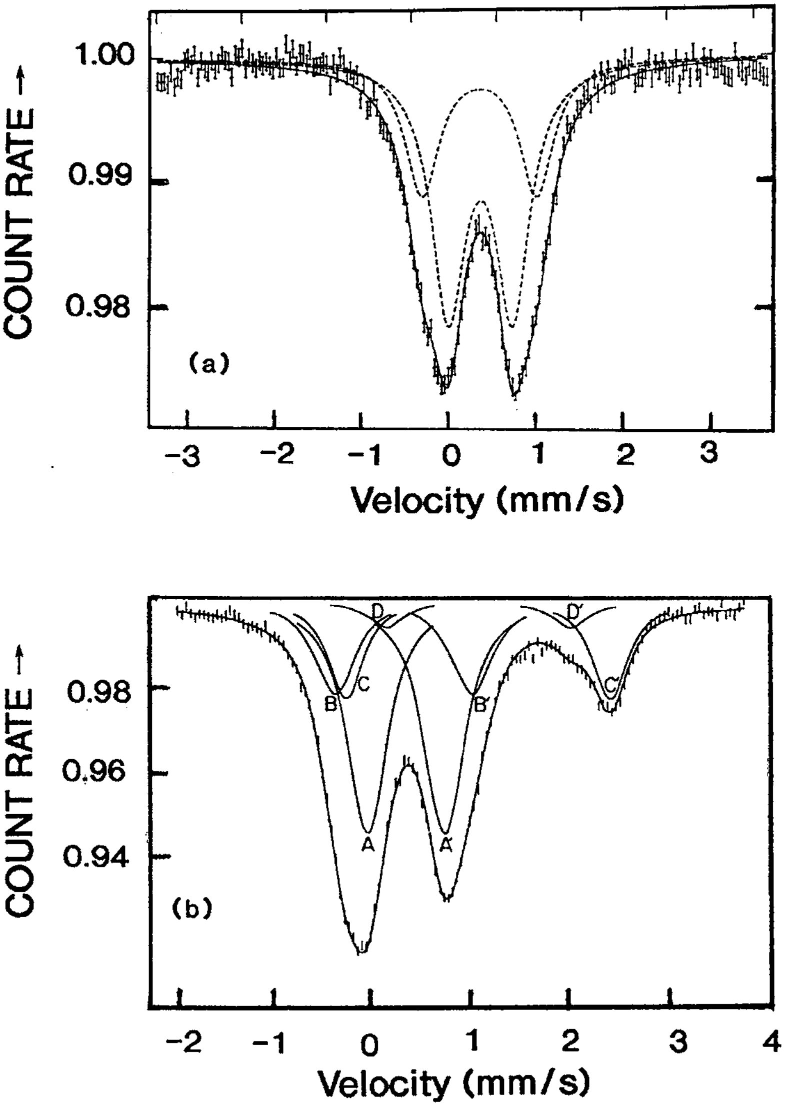

FIG. 4. ^{57}Fe Mössbauer spectra of synthetic magnesio-hastingsite: (a) synthesized on the CT (cuprite – tenorite) buffer; outer doublet: Fe^{3+} at *M*(2); inner doublet: Fe^{3+} at *M*(1) + *M*(3); (b) synthesized on the CCO (carbon – carbon monoxide) buffer; AA′: Fe^{3+} at *M*(2); BB′: Fe^{3+} at *M*(1) + *M*(3); CC′: Fe^{2+} at *M*(1) + *M*(3); DD′: Fe^{2+} at *M*(2); after Semet (1973).

member hastingsite, compared with values ranging from 0.12 to 0.22 for synthetic hastingsite, with the Fe^{3+} content increasing with increasing oxygen fugacity of synthesis. This is in accord with the slight decrease in cell dimensions with increasing oxygen fugacity of synthesis recorded by Thomas (1982a). Thus on the QFM buffer, synthetic hastingsite does contain the ideal amount of Fe^{3+}, but there is no information as to the relative ordering of Fe^{2+} and Fe^{3+} over *M*(1), *M*(2) and *M*(3), except for the fact that the Mössbauer spectra cannot be satisfactorily interpreted in terms of an ideal ordered model.

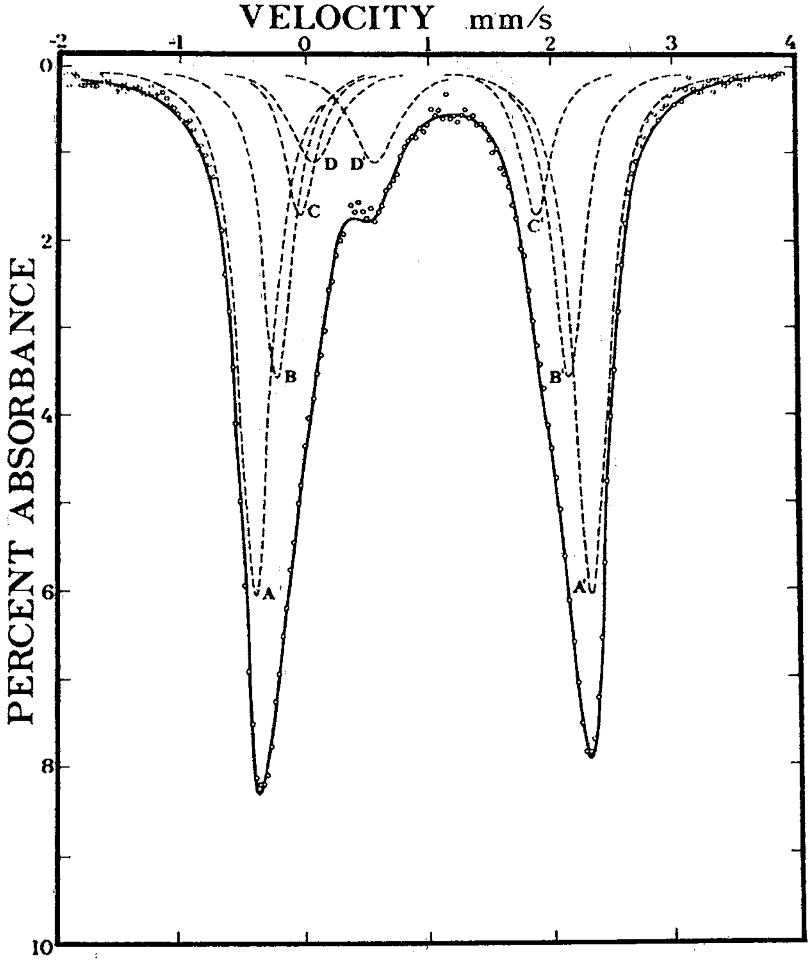

FIG. 5. The ^{57}Fe Mössbauer spectrum of synthetic hastingsite; after Thomas (1982b). Doublets AA′, BB′ and CC′ are assigned to Fe^{2+}, doublet DD′ is assigned to Fe^{3+}.

SODIC–CALCIC AMPHIBOLES

Richterite

Richterite and various substituted analogues are the most extensively investigated of the synthetic amphiboles. Richterite, ideally $NaCaNaMg_5Si_8O_{22}(OH)_2$, has been synthesized by Phillips & Rowbotham (1968), Huebner & Papike (1970), Forbes (1971), Charles (1974, 1975, 1977), Raudsepp *et al.* (1991) and Robert *et al.* (1989). Reported yields are usually very high: 98–100% (Charles 1974) and "essentially 100% pure" (Charles 1975).

From visual examination of run products, richterite seems to be the composition that gives the highest yield of amphibole. Cell dimensions are consistent throughout the numerous studies, suggesting good reproducibility. However, the infrared spectrum in the principal OH-stretching region (Fig. 6) indicates that synthetic richterite does deviate from its ideal composition. End-member richterite should give a single principal OH-stretching band due to the local configuration Mg_3–OH–^{A}Na. Considerable spectroscopic work (Rowbotham & Farmer 1973, Raudsepp 1984, Robert *et al.* 1989) has led to the assignment of the 3725 cm^{-1} band (Fig. 6) to this configuration. However, the spectrum contains another, weaker band at 3670 cm^{-1}; this stretching frequency corresponds very closely to that observed in tremolite (Hawthorne & Grundy 1976) and is generally assigned to the local configuration Mg_3–OH–$^A\square$. The spectrum indicates

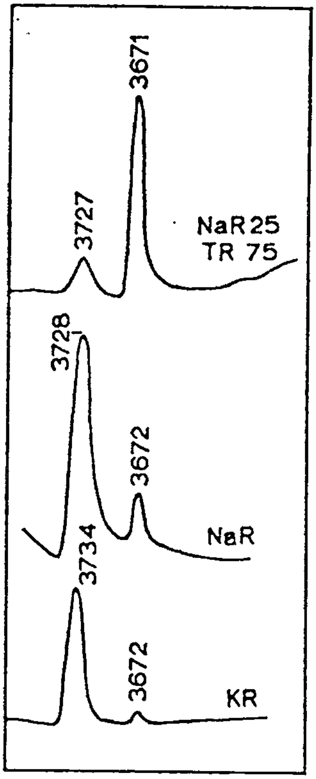

FIG. 6. Infrared spectra in the principal OH-stretching region for synthetic richterite amphiboles; KR = potassium-richterite, NaR = richterite, NaR25TR75 = solid solution of 25% richterite and 75% tremolite; after Rowbotham & Farmer (1973).

significant vacancy at the *A* site in synthetic richterite, presumably compensated by a similar deficiency of Na and corresponding excess of Ca at the *M*(4) site. Thus synthetic richterite deviates from the end-member composition, with Na–□ disorder at the *A* site.

Potassium-richterite

Potassium-richterite has been synthesized by Phillips & Rowbotham (1968), Huebner & Papike (1970), Raudsepp *et al.* (1991) and Della Ventura *et al.* (1991, 1993). As with richterite, the infrared spectrum in the principal OH-stretching region shows a band at ~3670 cm^{-1} (Fig. 6), indicative of significant vacancy at the *A* site, albeit not as much as occurs in richterite (which has Na at the *A* site). Natural potassium-richterite shows the same feature. Della Ventura *et al.* (1983) and Mottana & Griffen (1986) reported infrared spectra for natural samples, all of which show a significant 3670 cm^{-1} band indicative of vacancy at the *A* site.

Ferro-richterite

Ferro-richterite has been synthesized and well characterized by Charles (1974, 1975, 1977). Run products were shown to contain a significant amount (10–30%) of additional phases, usually clinopyroxene, fayalite and glass, and the amount of non-amphibole phases in the run products increases steadily across the series from zero (or close to zero) for richterite to up to 30% for ferro-richterite. Figure 7 shows the variation in cell volume across the series synthesized on the iron–wüstite buffer. Two varieties of ferro-richterite are shown. The variety with the lower cell volume was synthesized at 500–530°C for 22–30 days, with an amphibole yield of >95% plus clinopyroxene, olivine and clear glass. The variety with the higher cell volume was synthesized at 600–700°C for <10 days, with an amphibole yield of 90% plus clinopyroxene, olivine and a trace of glass. The nonlinear behavior of the cell volume in the lower-temperature amphibole is indicative of the occurrence of Fe^{3+} in the structure, as confirmed by Mössbauer spectroscopy (Fig. 8). However, both Virgo (1972) and Charles (1974) stated that Mössbauer spectroscopy showed that *all* Fe-bearing amphiboles across the join contain Fe^{3+}, even though they were synthesized at low oxygen fugacities (iron–wüstite buffer). Thus synthetic ferro-richterite contains significant Fe^{3+} and therefore must be off-composition in other (unspecified) ways. Both of these features introduce significant disorder into an ideally well-ordered structure.

DISCUSSION

The importance of configurational entropy in amphibole stability has been considered by Westrich & Holloway (1981), Graham & Navrotsky (1986), Graham *et al.* (1989) and Welch *et al.* (1994). All of these authors showed that different patterns of order can lead to large differences in configurational entropy, which can dramatically affect the (calculated) stability of an amphibole. This suggests the reason for the observed difficulty in synthesizing ordered end-member amphiboles and in finding their natural analogues. An intermediate-composition amphibole, such as pargasite of composition $NaCa_2Mg^{2+}_{2.0}Fe^{2+}_{2.0}Al_{1.0}(Si_6Al_2)O_{22}(OH)_2$, has mixing of Mg and Fe^{2+} over the three octahedrally coordinated sites in the structure, with a significant contribution of configurational entropy to its total entropy. This term becomes less significant as the amount of Fe^{2+} in the structure decreases, and the contribution due to Mg–Fe^{2+}

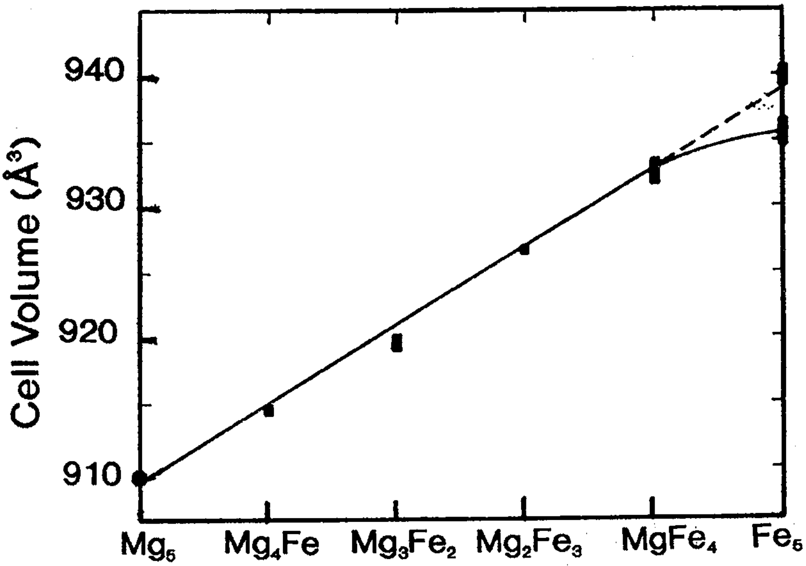

FIG. 7. Unit-cell volume of synthetic amphibole along the richterite–ferro-richterite join and synthesized on the I–W buffer (after Charles 1974).

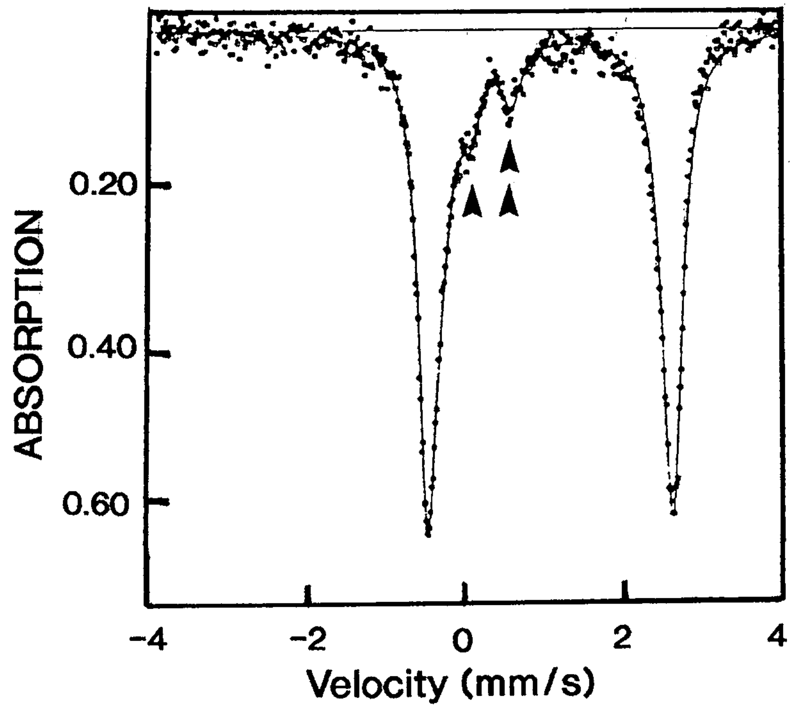

FIG. 8. The ^{57}Fe Mössbauer spectrum of synthetic ferro-richterite synthesized on the I–W buffer; black arrows mark the positions of a quadrupole-split Fe^{3+} doublet; after Virgo (1972).

disorder vanishes at the ideal end-member composition, having a destabilizing effect on the amphibole. However, this may be compensated by inducing Mg–Al disorder over the octahedral sites [actually over the *M*(2) and *M*(3) sites], which provides a new contribution of configurational entropy to the energetics of the structure. As emphasized by Navrotsky (1994), a little entropy goes a long way, and the TΔS term is very influential in mineral stability at high temperature. I suggest that it is here that one can find the reason for departures from ideal compositions and from ordered arrangements of cations in synthetic nominal end-member amphiboles. There has been a significant amount of work that has addressed the composition of synthetic tremolite, and there is a considerable amount of information available on the degree of order in pargasite and substituted pargasites. These two examples are considered in detail below.

Tremolite

Graham *et al.* (1989) and Welch & Pawley (1991) have suggested an interpretation of the phase relations of tremolite that is slightly different from that of Jenkins (1987). From the compositions of (natural) tremolite, they proposed that ideal end-member tremolite is stable at low temperature and with increasing temperature, starts to "break down" divariantly, with the tremolite becoming more magnesian during its breakdown (Graham *et al.* 1989). A schematic T–*X* section is shown in Figure 1b. The difference between the proposals of Jenkins (1987) and Graham *et al.* (1989) hinge on the composition at which the field of stability for tremolite exists at low temperature: Jenkins (1987) proposed that it does not encompass the ideal end-member tremolite composition, whereas Graham *et al.* (1989) proposed that it does include this composition. However, these differences do *not* change the fact that the composition of synthetic tremolite is affected by incongruent dissolution that is controlled by the solubility of silica in the ambient fluid (Jenkins *et al.* 1991).

There are three possibilities with regard to the magnesio-cummingtonite component in tremolite: (1) it is randomly distributed throughout the tremolite structure as $^{M(4)}$Mg, (2) there is some kind of medium-range order whereby domains of magnesio-cummingtonite occur within tremolite, and (3) there are intergrowths of (or defects involving) a more Mg-rich pyribole structure within the tremolite structure. Ahn *et al.* (1991) showed that chain-width defects (called CMFs, chain-multiplicity faults, by Maresch & Czank 1983a) are widespread in synthetic tremolite. The density of CMFs is inversely related to the temperature of synthesis, and Ahn *et al.* (1991) suggested that triple-chain silicate may be an important precursor to tremolite during the synthesis process. These results were amplified by Maresch *et al.* (1994), who showed that the nature of the amphibole microstructures depends on growth mechanisms, which differ as a function of temperature and pressure. At P(H_2O) less than 10 kbar, tremolite forms by topotactic reaction from metastable talc, and CMFs are common. At P(H_2O) greater than or equal to 10 kbar, amphibole grows topotactically from (and nucleates preferentially on) metastable diopside; fine lamellar intergrowths of tremolite and diopside occur, and triple or higher CMFs are rare. Thus it is apparent that point (3) (see above) is of major importance in this issue. Does the presence of CMFs account completely for the magnesio-cummingtonite component in tremolite? Ahn *et al.* (1991) concluded that (3) is insufficient to account completely for the low Ca/Mg value in synthetic tremolite, and estimated 5% occupancy of *M*(4) by Mg in a synthetic tremolite. Maresch *et al.* (1994) stated that "Our tremolitic amphiboles of *P*/*T* region I (T less than or equal to 750°C, P(H_2O) less than 10 kbar) do not require the assumption of a solid-solution toward magnesio-cummingtonite to interpret product assemblages and phase relations". On the other hand, Pawley *et al.* (1993) reported "only a few" CMFs in tremolite synthesized from a composition tremolite$_{(92)}$magnesio-cummingtonite$_{(8)}$, but could not resolve whether or not the CMFs involve single- or triple-chains. Bozhilov *et al.* (1993) reported a progressive decrease in the density of CMFs with increased annealing time at T = 850°C and P(H_2O) = 6.1 kbar.

From the above discussion, it is apparent that more than one factor is operative in affecting the composition of synthetic tremolite. First, there seems to be a kinetic problem whereby residual CMFs from a precursor phase are present (Ahn *et al.* 1991, Maresch *et al.* 1994), and their density decreases with increasing temperature of synthesis and increasing time of annealing (Ahn *et al.* 1991, Bozhilov *et al.* 1993). There are three possibilities here: (1) the reaction can go to completion with the synthesis of nominal end-member tremolite, (2) the reaction can go to completion with the synthesis of an equilibrium tremolite$_{(\sim 90)}$magnesio-cummingtonite$_{(\sim 10)}$, or (3) exchange of components with the external medium becomes kinetically inhibited by the progressive decrease in defect density, and either (a) a residual density of CMFs occur to give a composition with a significant magnesio-cummingtonite component, or (b) the excess Mg initially resident in residual CMFs goes into solid solution with tremolite [*i.e.*, Mg occupies the *M*(4) site], producing a homogeneous phase that may be stable or metastable. Taken by themselves, the HRTEM data and the above possibilities all indicate that if nominal tremolite is the equilibrium phase, the composition of synthesis products should converge on the nominal tremolite composition (or a minimal magnesio-cummingtonite component) with increasing temperature of synthesis and increasing time of annealing. The phase relations proposed by both

Jenkins (1987) and Graham *et al.* (1989) are not compatible with the above statement, as both schemes indicated *increased* magnesio-cummingtonite component (whatever the structural form it takes) with *increasing* temperature. This suggests that although the density of CMFs decreases with increasing temperature, the synthesis is converging on a composition that is *not* that of nominal tremolite [*i.e.*, situation (3a) or (3b) above].

The above discussion concerns the *mechanism* by which synthetic tremolite grows, and the structural nature of the way in which its bulk composition departs from that of nominal end-member tremolite. It is apparent that there are significant kinetic effects whereby the synthesis reaction commonly does not go to completion. However, it still seems that synthetic tremolite does not have nominal composition, even taking into account residual CMFs, or the compositional stability field of tremolite would converge toward the nominal composition with increasing temperature, rather than diverge as indicated by Jenkins (1987) and Graham *et al.* (1989). Thus one is still left with the challenge of finding the reason *why* synthetic tremolite is not of nominal composition. For a composition tremolite$_{(90)}$magnesio-cummingtonite$_{(10)}$, $M(4) = 0.90\text{Ca} + 0.10\text{Mg}$ if the magnesio-cummingtonite component is randomly distributed in solid solution with the tremolite. The resulting configurational entropy may be written as

$$S_{\text{conf}} = -R\Sigma_i\Sigma_j X_{ij}\ln X_{ij} \qquad (3)$$

in which the species j are distributed over the sites i. For the above situation $S_{conf} = -2R[0.90\ln0.90 + 0.10\ln0.10] = 5.4$ J/mol·K. Thus the observed departure from ideal end-member composition will produce a significant decrease in the free energy of the amphibole.

Pargasite

Synthetic pargasite, natural Fe-poor pargasite and synthetic M^{3+}-substituted pargasite all show significant M^{3+} disorder over the $M(2)$ and $M(3)$ sites. With increasing substitution of other divalent cations (*e.g.*, Fe^{2+}, Co) for Mg, this disorder decreases strongly. Thus compositions at, or close to, the nominal end-member composition show much more Mg–M^{3+} disorder than intermediate compositions. Does this disorder lead to a significant gain in configurational entropy? Ideal ordered end-member pargasite has $M(1) = M(3) = \text{Mg}$, $M(2) = 1.0\text{Al} + 1.0\text{Mg}$, with a resulting S_{conf} of $-2R[0.50\ln0.50 + 0.50\ln0.50] = 11.5$ J/mol·K. Synthetic end-member pargasite has $M(1) = \text{Mg}$, $M(2) = 0.25\text{Al} + 0.75\text{Mg}$, $M(3) = 0.50\text{Mg} + 0.50\text{Al}$, with a resulting S_{conf} of $-R[2(0.25\ln0.25 + 0.75\ln0.75) + (0.5\ln0.50 + 0.5\ln0.50)] = 15.1$ J/mol·K. Thus the disordered synthetic pargasite has a relative stabilization due to configurational entropy of 3.6 J/mol.K compared to its ordered analogue. Of course, both synthetic end-member pargasite and its hypothetical Mg–Al ordered analogue have additional configurational entropy terms involving Al–Si at the $T(1)$ and $T(2)$ sites and Na at the $A(2)$ site, plus potential contributions resulting from short-range order, but these will not necessarily contribute to the *difference* in configurational entropy between the two arrangements.

As noted above, the amount of Al disorder over the $M(2)$ and $M(3)$ sites in pargasite decreases with increasing substitution of other divalent cations for Mg. Although such substitutions will usually lead to an increase in configurational entropy due to Mg,M^{2+} disorder, another effect is also apparent. Mg is always replaced by larger divalent cations, and hence there may be an effect of cation size on ordering. Furthermore, Mg is always replaced by a transition metal with unfilled *d*-orbitals, and hence additional electronic effects may be operative. Della Ventura *et al.* (1995) report the synthesis and characterization of nominal $NaCa_2(Co_4^{2+}Al)(Si_6Al_2)O_{22}(OH)_2$ and show by infrared spectroscopy and Rietveld structure refinement that $^{[6]}$Al is completely ordered at the $M(2)$ site. Thus either increasing $^{[6]}M^{2+}$ cation size or changing electronic structure reduces $^{[6]}$Al disorder over the $M(2)$ and $M(3)$ sites in the pargasite structure. So what happens to the configurational entropy in Co^{2+}-pargasite? The amphibole yield for the nominal pargasite composition is ~98% (Charles 1980, Raudsepp *et al.* 1987a, 1991, Welch *et al.* 1994), whereas Della Ventura *et al.* (1995) report the amphibole yield for nominal Co^{2+}-pargasite as ~90% with coexisting Co^{2+}-diopside and anorthite (plagioclase). The phase assemblage produced during Co^{2+}-pargasite synthesis indicates that the Co^{2+}-pargasite produced must be richer in Co^{2+} and poorer in Ca than the nominal composition. Furthermore, the Rietveld refinement of Della Ventura *et al.* (1995) shows that $M(2) = 1.02Co^{2+} + 0.98\text{Al}$, *i.e.*, the ideal site-population for ideal ordered Co^{2+}–pargasite; hence any excess Co^{2+} in Co^{2+}–pargasite does not occur at the $M(1)$, $M(2)$ or $M(3)$ sites. The phase assemblage and the $M(2)$ site population indicate that there must be significant replacement of Ca by Co^{2+} at the $M(4)$ site. In this regard, Oberti *et al.* (1995a) report significant occupancy of the $M(4)$ site by Mn^{2+},Fe^{2+} in pargasite crystals from the Finero complex. Thus, although synthetic Co^{2+}-pargasite does not show the extensive Al disorder over $M(2)$ and $M(3)$ typical of synthetic pargasite, it does show Ca,Co^{2+} disorder at the $M(4)$ site.

CONCLUSIONS

I propose that end-member or close-to-end-member amphiboles commonly show entropy-driven disorder that is required for their occurrence as stable structures.

This disorder may occur as unusual site-populations, as small deviations from ideal end-member composition, or even possibly as stacking disorder, as occurs for the Fe–Mn–Mg amphiboles (Maresch & Czank 1983a, b, 1988). I realize that this idea is rather speculative. However, it does tie together a large number of otherwise disparate and unconnected observations. Although it cannot be categorically stated that completely ordered end-member amphiboles of ideal composition never occur, I suggest that it is our own sense of order that has led us to believe that such ideal minerals should always exist; the experimental evidence often seems to suggest otherwise.

ACKNOWLEDGEMENTS

I am very grateful to Dave Jenkins and Mark Welch for their comments on this manuscript. The work was supported by the Natural Sciences and Engineering Research Council of Canada in the form of an Operating grant to FCH.

REFERENCES

AHN, J.H., CHO, M., JENKINS, D.M. & BUSECK, P.R. (1991): Structural defects in synthetic tremolitic amphiboles. *Am. Mineral.* **76**, 1811-1823.

BOSCHMANN, K.F., BURNS, P.C., HAWTHORNE, F.C., RAUDSEPP, M. & TURNOCK, A.C. (1994): A-site disorder in synthetic fluor-edenite, a crystal-structure study. *Can. Mineral.* **32**, 21-30.

BOYD, F.R. (1959): Hydrothermal investigations of amphiboles. *In* Researches in Geochemistry (P.H. Abelson, ed.). John Wiley & Sons, New York (377-396).

BOZHILOV, K., JENKINS, D.J. & VEBLEN, D.R. (1993): TEM/AEM observations on chain silicate evolution during synthesis of tremolite. *Am. Geophys. Union, Trans. (Eos)* **74**, 166 (abstr.).

BURNS, R.G. & GREAVES, C.J. (1971): Correlations of infrared and Mössbauer site population measurements of actinolites. *Am. Mineral.* **56**, 2010-2033.

CAMERON, M. & GIBBS, G.V. (1973): The crystal structure and bonding of fluor-tremolite: a comparison with hydroxyl tremolite. *Am. Mineral.* **58**, 879-888.

CHARLES, R.W. (1974): The physical properties of the Mg–Fe richterites. *Am. Mineral.* **59**, 519-528.

________ (1975): The phase equilibria of richterite and ferrorichterite. *Am. Mineral.* **60**, 367-374.

________ (1977): The phase equilibria of intermediate compositions on the pseudobinary $Na_2CaMg_5Si_8O_{22}(OH)_2$ – $Na_2CaFe_5Si_8O_{22}(OH)_2$. *Am. J. Sci.* **277**, 594-625.

________ (1980): Amphiboles on the join pargasite – ferropargasite. *Am. Mineral.* **65**, 996-1001.

CHO, M. & ERNST, W.G. (1991): An experimental determination of calcic amphibole solid solution along the join tremolite–tschermakite. *Am. Mineral.* **76**, 985-1001.

DELLA VENTURA, G., MARAS, A. & PARODI, G.C. (1983): Potassium-fluorrichterite from Monte Somma (Campania, Italy). *Per. Mineral. (Roma)* **52**, 617-630.

________, ROBERT, J.-L. & BÉNY, J.-M. (1991): Tetrahedrally coordinated Ti^{4+} in synthetic Ti-rich potassic richterite: evidence from XRD, FTIR and Raman studies. *Am. Mineral.* **76**, 1134-1140.

________, ________, ________, RAUDSEPP, M. & HAWTHORNE, F.C. (1993): The OH–F substitution in Ti-rich potassium-richterite: Rietveld structure refinement and FTIR and micro-Raman spectroscopic studies of synthetic amphiboles in the system $K_2O–Na_2O–CaO–MgO–SiO_2–TiO_2–H_2O–HF$. *Am. Mineral.* **78**, 980-987.

________, ________, HAWTHORNE, F.C. & RAUDSEPP, M. (1995): Contrasting $^{[6]}Al$ ordering in synthetic Mg- and Co-pargasite. *Eur. J. Mineral.* (accepted).

ERNST, W.G. (1966): Synthesis and stability relations of ferro-tremolite. *Am. J. Sci.* **264**, 37-65.

________ (1968): *Amphiboles: Crystal Chemistry, Phase Relations, and Occurrence.* Springer-Verlag, New York, N.Y.

FORBES, W.C. (1971): Synthesis and stability relations of richterite, $Na_2CaMg_5Si_8O_{22}(OH)_2$. *Am. Mineral.* **56**, 997-1004.

GILBERT, M.C. (1966): Synthesis and stability relations of the hornblende ferropargasite. *Am. J. Sci.* **264**, 698-742.

GRAHAM, C.M., MARESCH, W.V., WELCH, M.D. & PAWLEY, A.R. (1989): Experimental studies on amphiboles: a review with thermodynamic perspectives. *Eur. J. Mineral.* **1**, 535-555.

________ & NAVROTSKY, A. (1986): Thermochemistry of the tremolite–edenite amphiboles using fluorine analogues, and applications to amphibole – plagioclase – quartz equilibria. *Contrib. Mineral. Petrol.* **93**, 18-32.

HAWTHORNE, F.C. (1983): Characterization of the average structure of natural and synthetic amphiboles. *Per. Mineral. (Roma)* **52**, 543-581.

________ & GRUNDY, H.D. (1976): The crystal chemistry of the amphiboles. IV. X-ray and neutron refinements of the crystal structure of tremolite. *Can. Mineral.* **14**, 334-345.

________, OBERTI, R., UNGARETTI, L. & GRICE, J.D. (1995): Fluor-cannilloite: a new hyper-calcic amphibole from Pargas, Finland with Ca at the A site. *Am. Mineral.* (in press).

HUEBNER, J.S. & PAPIKE, J.J. (1970): Synthesis and crystal chemistry of sodium-potassium richterite, (Na,K)

$NaCaMg_5Si_8O_{22}(OH,F)_2$: a model for amphiboles. *Am. Mineral.* **55**, 1973-1992.

JENKINS, D.M. (1987): Synthesis and characterization of tremolite in the system H_2O–CaO–MgO–SiO_2. *Am. Mineral.* **72**, 707-715.

________, HOLLAND, T.J.B. & CLARE, A.K. (1991): Experimental determination of the pressure-temperature stability field and thermochemical properties of synthetic tremolite. *Am. Mineral.* **76**, 458-469.

KISELEVA, I.A. & OGORODOVA, L.P. (1984): High-temperature solution calorimetry for determining the enthalpies of formation for hydroxyl-containing minerals such as talc and tremolite. *Geochem. Int.* **21**, 36-46.

MARESCH, W.V. & CZANK, M. (1983a): Problems of compositional and structural uncertainty in synthetic hydroxy-amphiboles; with an annotated atlas of the realbau. *Per. Mineral. (Roma)* **52**, 463-542.

________ & ________ (1983b): Phase characterization of synthetic amphiboles on the join $Mn_x^{2+}Mg_{7-x}Si_6O_{22}(OH)_2$. *Am. Mineral.* **68**, 744-753.

________ & ________ (1988): Crystal chemistry, growth kinetics and phase relationships of structurally disordered (Mn^{2+},Mg)-amphiboles. *Fortschr. Mineral.* **66**, 69-121.

________, ________ & SCHREYER, W. (1994): Growth mechanisms, structural defects and composition of synthetic tremolite: what are the effects on macroscopic properties? *Contrib. Mineral. Petrol.* **118**, 297-313.

MOTTANA, A. & GRIFFIN, W.L. (1986): Crystal chemistry of two coexisting K-richterites from St. Marcel (Val d'Aosta, Italy). *Am. Mineral.* **71**, 1426-1433.

NAVROTSKY, A. (1994): Repeating patterns in mineral energetics. *Am. Mineral.* **79**, 589-605.

OBA, T. (1980): Phase relations in the tremolite–pargasite join. *Contrib. Mineral. Petrol.* **71**, 247-256.

OBERTI, R., HAWTHORNE, F.C., UNGARETTI, L. & CANNILLO, E. (1995a): $^{[6]}$Al disorder in amphiboles from mantle peridotites. *Can. Mineral.* **33**, 867-878.

________, SARDONE, R., HAWTHORNE, F.C., RAUDSEPP, M. & TURNOCK, A. (1995b): Synthesis and crystal-structure refinement of synthetic fluor-pargasite. *Can. Mineral.* **33**, 25-31.

PAWLEY, A.R., GRAHAM, C.M. & NAVROTSKY, A. (1993): Tremolite-richterite amphiboles: synthesis, compositional and structural characterization, and thermochemistry. *Am. Mineral.* **78**, 23-35.

PHILLIPS, R. & ROWBOTHAM, G. (1968): Studies on synthetic alkali amphiboles. *Papers and Proceedings of the Fifth General Meeting, Int. Mineral. Assoc. (Cambridge)*, 249-254.

RAUDSEPP, M. (1984): *Evaluation of Amphibole Synthesis and Product Characterization.* Ph.D. thesis, Univ. Manitoba, Winnipeg, Manitoba.

________, TURNOCK, A.C. & HAWTHORNE, F.C. (1987b): Characterization of cation ordering in synthetic scandium-fluor-eckermannite, indium-fluor-eckermannite and scandium-fluor-nyböite by Rietveld structure refinement. *Am. Mineral.* **72**, 959-964.

________, ________ & ________ (1991): Amphibole synthesis at low-pressure: what grows and what doesn't. *Eur. J. Mineral.* **3**, 983-1004.

________, ________, ________, SHERRIFF, B.L. & HARTMAN, J.S. (1987a): Characterization of synthetic pargasitic amphiboles ($NaCa_2Mg_4M^{3+}Si_6Al_2O_{22}(OH,F)_2$; M^{3+} = Al, Cr, Ga, Sc, In) by infrared spectroscopy, Rietveld structure refinement and ^{27}Al, ^{29}Si, and ^{19}F MAS NMR spectroscopy. *Am. Mineral.* **72**, 580-593.

ROBERT, J.-L., DELLA VENTURA, G. & THAUVIN, J.-L. (1989): The infrared OH-stretching region of synthetic richterites in the system $Na_2O - K_2O - CaO - MgO - SiO_2 - H_2O -$ HF. *Eur. J. Mineral.* **1**, 203-211.

ROWBOTHAM, G. & FARMER, V.C. (1973): The effect of "A" site occupancy on the hydroxyl stretching frequency in clinoamphiboles. *Contrib. Mineral. Petrol.* **38**, 147-149.

SEMET, M.P. (1973): A crystal-chemical study of synthetic magnesiohastingsite. *Am. Mineral.* **58**, 480-494.

SKIPPEN, G. & MCKINSTRY, B.W. (1985): Synthetic and natural tremolite in equilibrium with forsterite, enstatite, diopside, and fluid. *Contrib. Mineral. Petrol.* **89**, 256-262.

THOMAS, W.M. (1982a): Stability relations of the amphibole hastingsite. *Am. J. Sci.* **282**, 136-164.

________ (1982b): ^{57}Fe Mössbauer spectra of natural and synthetic hastingsites, and implications for peak assignments in calcic amphiboles. *Am. Mineral.* **67**, 558-567.

TROLL, G. & GILBERT, M.C. (1972): Fluorine-hydroxyl substitution in tremolite. *Am. Mineral.* **57**, 1386-1403.

VIRGO, D. (1972): Preliminary fitting of ^{57}Fe Mössbauer spectra of synthetic Mg–Fe richterites. *Carnegie Inst. Wash. Year Book* **71**, 513-516.

WELCH, M.D. (1987): *Experimental Studies of Amphiboles in the System* $Na_2O - CaO - MgO - Al_2O_3 - SiO_2 - H_2O - SiF_4$ *and its Subsystems.* Ph.D. thesis, Univ. of Edinburgh, Edinburgh, U.K.

________, KOLODZIEJSKI, W. & KLINOWSKI, J. (1994): A multinuclear NMR study of synthetic pargasite. *Am. Mineral.* **79**, 261-268.

________ & PAWLEY, A.R. (1991): Tremolite: new enthalpy and entropy data from a phase equilibrium study of the reaction tremolite = 2diopside + 1.5orthoenstatite + β-quartz + H_2O. *Am. Mineral.* **76**, 1931-1939.

WESTRICH, H.R. & HOLLOWAY, J.R. (1981): Experimental dehydration of pargasite and calculation of its entropy and Gibbs energy. *Am. J. Sci.* **281**, 922-934.

——— & NAVROTSKY, A. (1981): Some thermodynamic properties of fluorapatite, fluorpargasite, and fluorphlogopite. *Am. J. Sci.* **281**, 1091-1103.

WONES, D.R. & DODGE, F.C.W. (1977): The stability of phlogopite in the presence of quartz and diopside. *In* Thermodynamics in Geology (D.G. Fraser, ed.). D. Reidel, Dordrecht, Holland (229-247).

Received August 3, 1994, revised manuscript accepted August 30, 1995.